Supporting Information for

How Could Future Climate Conditions Reshape a Devastating Lake-Effect Snow Storm?

Miraj B. Kayastha[1,2], Chenfu Huang[2], Jiali Wang[3], Yun Qian[4], Zhao Yang[4], TC Chakraborty[4], William J. Pringle[3], Robert D. Hetland[4], and Pengfei Xue[1,2,3]

[1]Department of Civil, Environmental, and Geospatial Engineering, Michigan Technological University, Houghton, MI, USA

[2]Great Lakes Research Center, Michigan Technological University, Houghton, MI, USA

[3]Environmental Science Division, Argonne National Laboratory, Lemont, IL, USA

[4]Pacific Northwest National Laboratory, Richland, WA, USA

Contents of this file

Introduction

The supplementary figures provide information about WRF-FVCOM and its simulation of the Buffalo LES storm under the warmer future conditions. The table provides the list of CMIP6 GCMs used for the PGW approach used in the study.
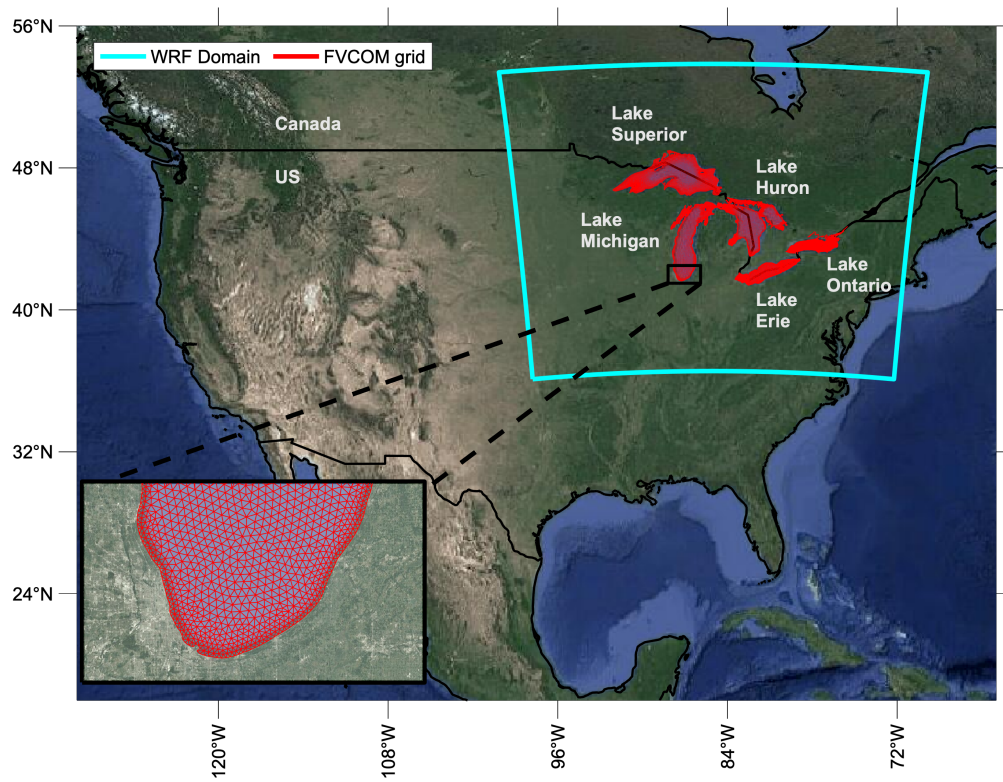
Figure S1. WRF-FVCOM domain. WRF's spatial domain along with FVCOM's unstructured triangular grid used to represent the Great Lakes.
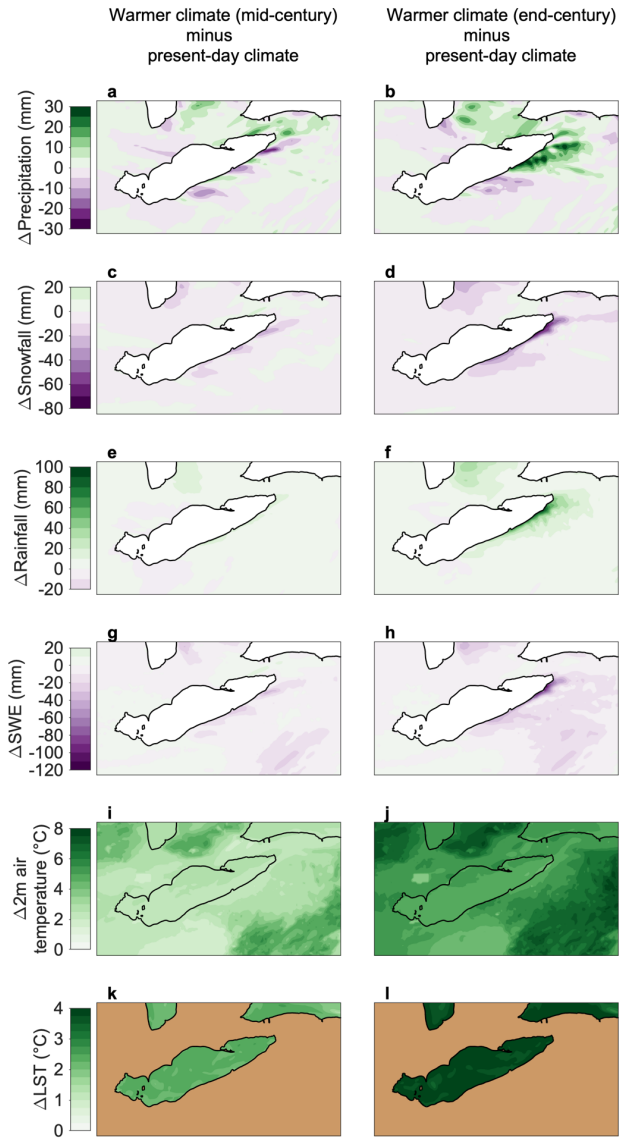
Figure S2. Spatial changes in storm conditions due to warmer future climates. Changes in the warmer future climates of mid-century and end-century relative to present-day climate for total precipitation (a,b), total snowfall (c,d), total rainfall (e,f), November 21 SWE (g,h), mean air temperature (i,j) and mean LST (k,l). The plotted values are the WRF-FVCOM's 10-member ensemble mean calculated for the November 16-21 period.
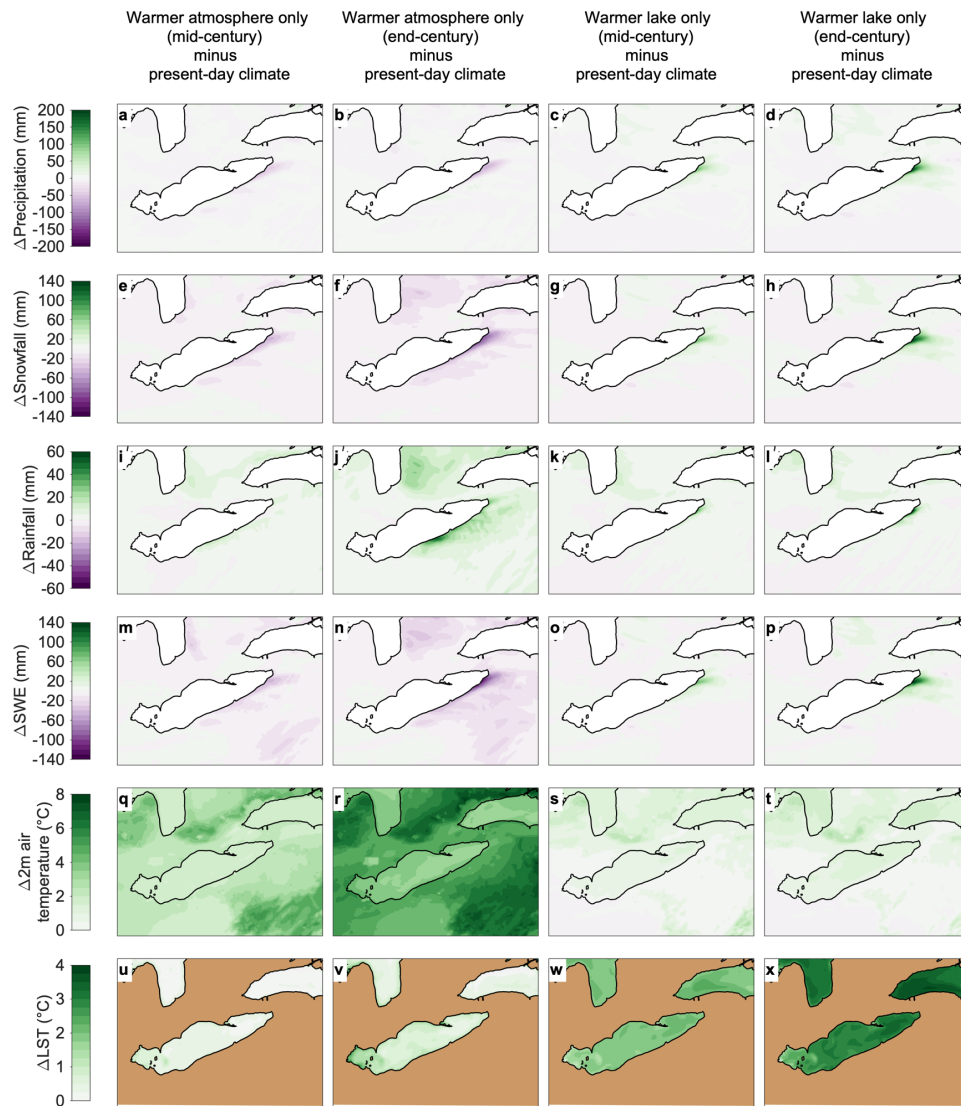
Figure S3. Spatial changes in storm conditions due to an isolated future warming of atmosphere and lake. Changes under various isolated future warming scenarios relative to present-day climate for total precipitation (a-d), total snowfall (e-h), total rainfall (i-l), November 21 SWE (m-p), mean air temperature (q-t), and mean LST (u-x). The plotted values are the WRF-FVCOM's 10-member ensemble mean calculated for the November 16-21 period.
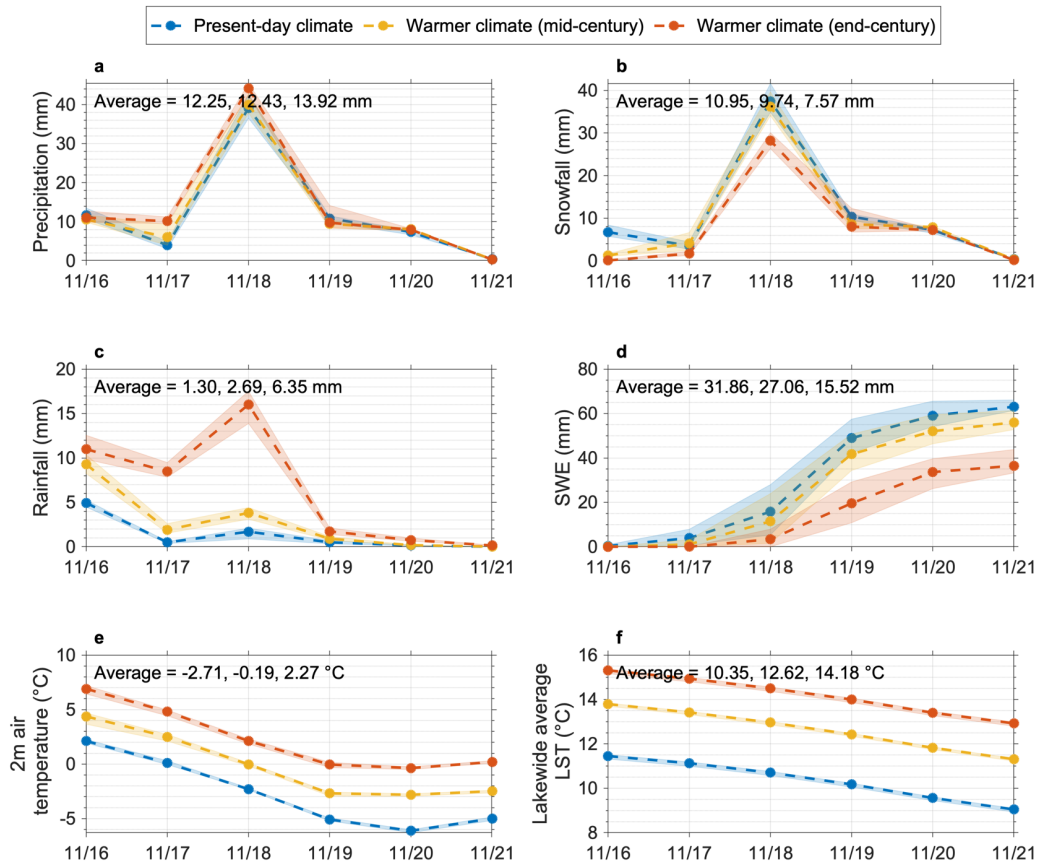
Figure S4. Temporal evolution of storm characteristics under warmer future climates. The temporal evolution under present-day climate and warmer future climates for precipitation (a), snowfall (b), rainfall (c), SWE (d), air temperature (e), and LST (f). The precipitation, snowfall, rainfall, SWE, and air temperature are averaged over Erie County. The LST is the lakewide average for Lake Erie. The average daily values under present-day climate, mid-century climate, and end-century climate are provided in each panel, in that order. The plotted values are the WRF-FVCOM's 10-member ensemble mean and the shading represents the ensemble range.

Figure S5. Temporal evolution of storm characteristics under isolated future warming of atmosphere and lake. The temporal evolution under present-day climate and various isolated future warming scenarios for precipitation (a), snowfall (b), rainfall (c), SWE (d), air temperature (e), and LST (f). The precipitation, snowfall, rainfall, SWE, and air temperature are averaged over Erie County. The LST is the lakewide average for Lake Erie. The average daily values under the present-day climate, isolated mid-century warming of the atmosphere, isolated end-century warming of the atmosphere, isolated mid-century warming of the lake, and isolated end-century warming of the lake are provided in each panel, in that order. The plotted values are the WRF-FVCOM's 10-member ensemble mean and the shading represents the ensemble range.
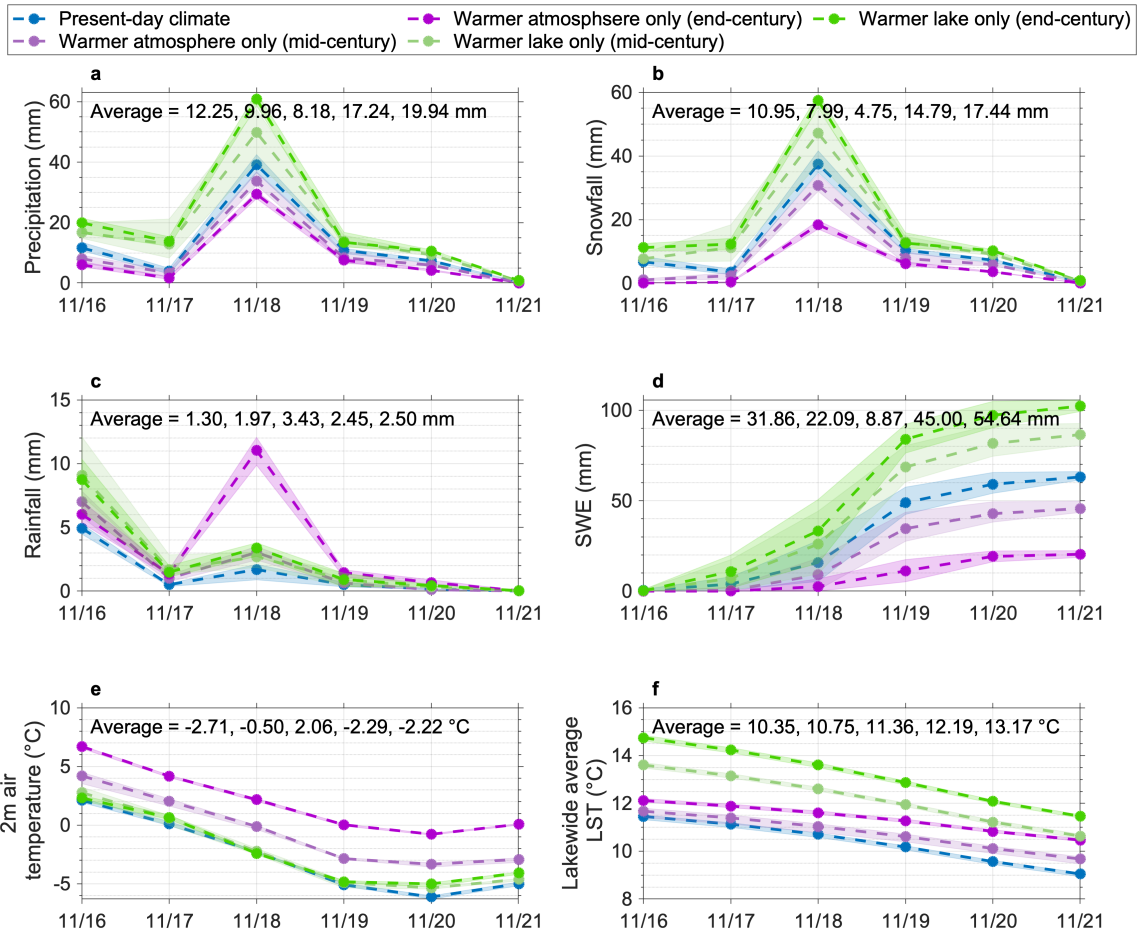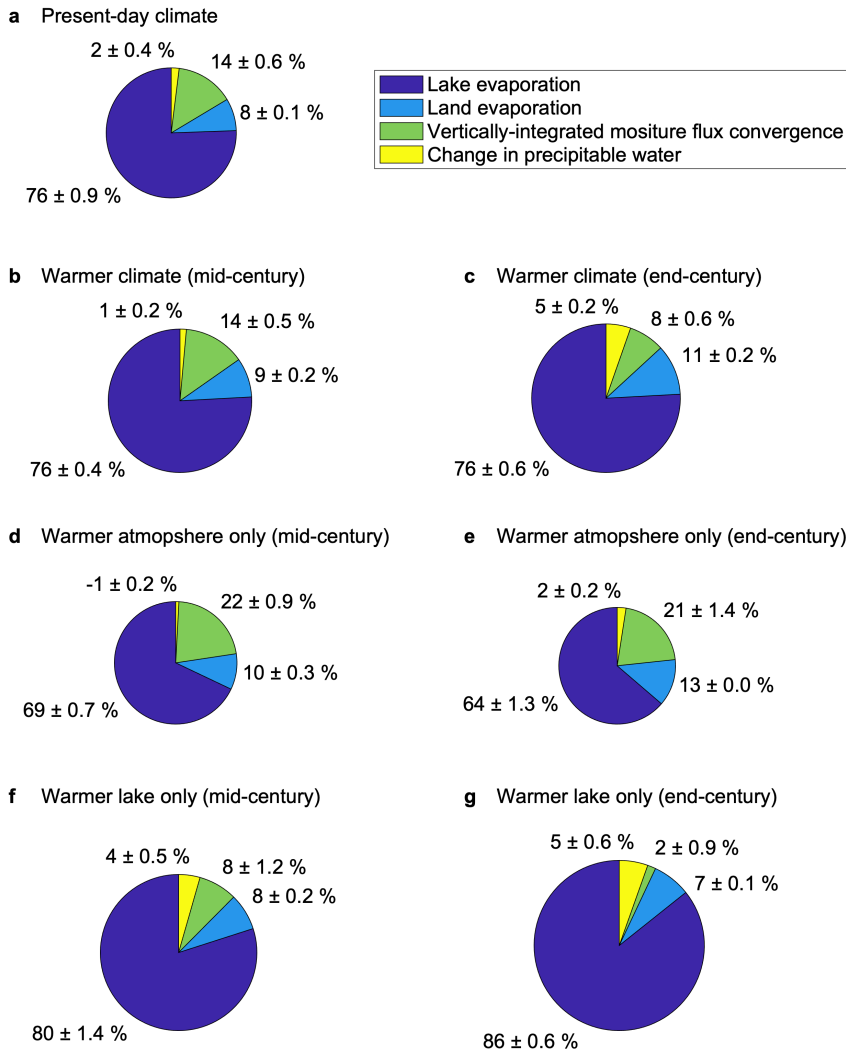
a Present-day climate

2 ± 0.4 % 14 ± 0.6 %
8 ± 0.1 %

Lake evaporation
Land evaporation
Vertically-integrated moisture flux convergence
Change in precipitable water

76 ± 0.9 %

b Warmer climate (mid-century)

1 ± 0.2 % 14 ± 0.5 %
9 ± 0.2 %

76 ± 0.4 %

c Warmer climate (end-century)

5 ± 0.2 % 8 ± 0.6 %
11 ± 0.2 %

76 ± 0.6 %

d Warmer atmopshere only (mid-century)

-1 ± 0.2 % 22 ± 0.9 %
10 ± 0.3 %

69 ± 0.7 %

e Warmer atmopshere only (end-century)

2 ± 0.2 % 21 ± 1.4 %
13 ± 0.0 %

64 ± 1.3 %

f Warmer lake only (mid-century)

4 ± 0.5 % 8 ± 1.2 %
8 ± 0.2 %

80 ± 1.4 %

g Warmer lake only (end-century)

5 ± 0.6 % 2 ± 0.9 %
7 ± 0.1 %

86 ± 0.6 %

Figure S6. Relative moisture contributions of moisture budget components to precipitation under various future warming scenarios. Relative moisture contributions to precipitation from lake evaporation, land evapotranspiration, vertically-integrated moisture flux convergence, and the change in precipitable water for various future warming scenarios. The results shown are the WRF-FVCOM's 10-member ensemble mean and standard deviation.

GCM	Spatial Resolution	Reference
ACCESS-CM2	1.25° x 1.88°	Bi et al. (2020)
CanESM5	2.79° x 2.81°	Swart et al. (2019)
FGOALS-f3-L	2.79° x 2.81	Zhou et al. (2014)
MIROC6	1.40° x1.41°	Tatebe et al. (2019)
CESM-WACCM	1.88° x 2.5°	Marsh et al. (2013)
E3SM-1-1	1° x 1°	Golaz et al. (2019)
GFDL-CM4	2.00° x 2.50°	Held et al. (2019)
MPI-ESM1-2-LR	1.86° x 1.88°	Jungclaus et al. (2013)
CMCC-CM2-SR5	0.75° x 0.75°	Cherchi et al. (2019)
IPSL-CM6A-LR	1.89° x 3.75°	Boucher et al. (2020)
NorESM2-LM	1.89° x 2.5°	Seland et al. (2020)

Table S1. CMIP6 GCMs used for PGW. List of CMIP6 GCMs used for the PGW approach to simulate the LES storm under various future warming scenarios.

References

Bi, D., Dix, M., Marsland, S., O'farrell, S., Sullivan, A., Bodman, R., . . . Rashid, H. A. (2020). Configuration and spin-up of ACCESS-CM2, the new generation Australian community climate and earth system simulator coupled model. *Journal of Southern Hemisphere Earth Systems Science, 70*(1), 225-251.

Boucher, O., Servonnat, J., Albright, A. L., Aumont, O., Balkanski, Y., Bastrikov, V., . . . Bopp, L. (2020). Presentation and evaluation of the IPSL-CM6A-LR climate model. *Journal of Advances in Modeling Earth Systems, 12*(7), e2019MS002010.

Cherchi, A., Fogli, P. G., Lovato, T., Peano, D., Iovino, D., Gualdi, S., . . . Bellucci, A. (2019). Global mean climate and main patterns of variability in the CMCC-CM2 coupled model. *Journal of Advances in Modeling Earth Systems, 11*(1), 185-209.

Golaz, J. C., Caldwell, P. M., Van Roekel, L. P., Petersen, M. R., Tang, Q., Wolfe, J. D., . . . Bader, D. C. (2019). The DOE E3SM coupled model version 1: Overview and evaluation at standard resolution. *Journal of Advances in Modeling Earth Systems, 11*(7), 2089-2129.

Held, I., Guo, H., Adcroft, A., Dunne, J., Horowitz, L., Krasting, J., . . . Bushuk, M. (2019). Structure and performance of GFDL's CM4. 0 climate model. *Journal of Advances in Modeling Earth Systems, 11*(11), 3691-3727.

Jungclaus, J. H., Fischer, N., Haak, H., Lohmann, K., Marotzke, J., Matei, D., . . . Von Storch, J. (2013). Characteristics of the ocean simulations in the Max Planck Institute Ocean Model (MPIOM) the ocean component of the MPI-Earth system model. *Journal of Advances in Modeling Earth Systems, 5*(2), 422-446.

Marsh, D. R., Mills, M. J., Kinnison, D. E., Lamarque, J.-F., Calvo, N., & Polvani, L. M. (2013). Climate change from 1850 to 2005 simulated in CESM1 (WACCM). *Journal of Climate, 26*(19), 7372-7391.

Seland, Ø., Bentsen, M., Olivié, D., Toniazzo, T., Gjermundsen, A., Graff, L. S., . . . Kirkevåg, A. (2020). Overview of the Norwegian Earth System Model (NorESM2) and key climate response of CMIP6 DECK, historical, and scenario simulations. *Geoscientific Model Development, 13*(12), 6165-6200.

Swart, N. C., Cole, J. N., Kharin, V. V., Lazare, M., Scinocca, J. F., Gillett, N. P., . . . Hanna, S. (2019). The Canadian earth system model version 5 (CanESM5. 0.3). *Geoscientific Model Development, 12*(11), 4823-4873.

Tatebe, H., Ogura, T., Nitta, T., Komuro, Y., Ogochi, K., Takemura, T., . . . Saito, F. (2019). Description and basic evaluation of simulated mean state, internal variability, and climate sensitivity in MIROC6. *Geoscientific Model Development, 12*(7), 2727-2765.

Zhou, T., Yu, Y., Liu, Y., & Wang, B. (2014). *Flexible global ocean-atmosphere-land system model: a modeling tool for the climate change research community*: Springer.